# Confocal Laser Scanning Microscopy: a new technique for investigating and illustrating fossil Radiolaria

**Barry O'Connor**
*Department of Geology, University of Auckland, Private Bag 92019, Auckland, New Zealand*

**ABSTRACT:** Confocal laser scanning microscopy (CLSM), a technique newly applied to the study of fossil Radiolaria, offers the radiolarist clear views of single optical planes of specimens, unhindered by many of the optical effects of conventional light microscopy, while obviating the need to section or break specimens. Resulting images are of a clarity unsurpassed by conventional light microscopy and, as they are saved on computer, are easily viewed, manipulated, enhanced, measured and converted to hard copy. Used in conjunction with common radiolarian study methods CLSM is a powerful tool for gaining additional information with relatively little extra effort.

## INTRODUCTION

Confocal laser scanning microscopy (CLSM) is a technique with which the microscopist can obtain clear views of single optical planes of a specimen without the optical effects of scatter (caused when light is reflected within the specimen in the plane of focus) or blur (due to light being reflected from above and below the plane of focus), ubiquitous with conventional light microscopy, and without having to destroy the specimen by sectioning, thus saving specimen and time. By eliminating scatter and blur the resulting image exhibits greater contrast and resolution and hence clarity. CLSM achieves this with three basic modifications to the conventional microscope (see text-fig.1).

**1.** Scatter is eliminated by focusing the excitation light (laser) to a point that intensely illuminates only a small spot of the specimen in the plane of focus, rather than illuminating the entire specimen as in conventional light microscopy. The resulting point of light may be as small as 0.25µm in diameter and 0.5µm deep.

**2.** The system eliminates blur by focusing returning emissions, caused by the excitation light, through a small aperture (or pinhole) enabling only those emissions from the plane of focus (ie. the area of interest) to be collected by the detector. This effectively produces a very small depth of field, somewhere in the range of 0.5-1.5µm. Due to these two modifications the excitation light, the specimen and the detector all have the same focus, ie. they are confocal.

**3.** Finally a rapidly pivoting mirror scans the point of light across the specimen (different systems use different scanning methods, eg. see Wright et al. 1993; Lichtman 1994). This is necessary as only a very small part of the specimen is illuminated at one time, so the entire area of interest must be scanned to build up an image. As each spot must be illuminated almost instantaneously and produce a detectable signal, a laser is used because it is very bright and easily focused to a point.

The use of a laser means that the light provided is actually excitation light, ie. it produces fluorescent emissions from its targets, rather than reflections as in conventional light microscopy. Depending upon the excitation wavelength of the laser, different dyes may be employed to stain particular parts of specimens so that they produce fluorescent emissions.

Overall, CLSM allows information to be collected from a well-defined optical section, rather than from most of the specimen as in conventional light microscopy. Images are stored on computer and can be readily studied and manipulated in graphical or image analysis software. For example, a series of optical sections taken at successive focal planes, ie. along the $z$ axis, within a specimen (called a $z$ series) can be reconstructed to form a three-dimensional representation which can be rotated for view-

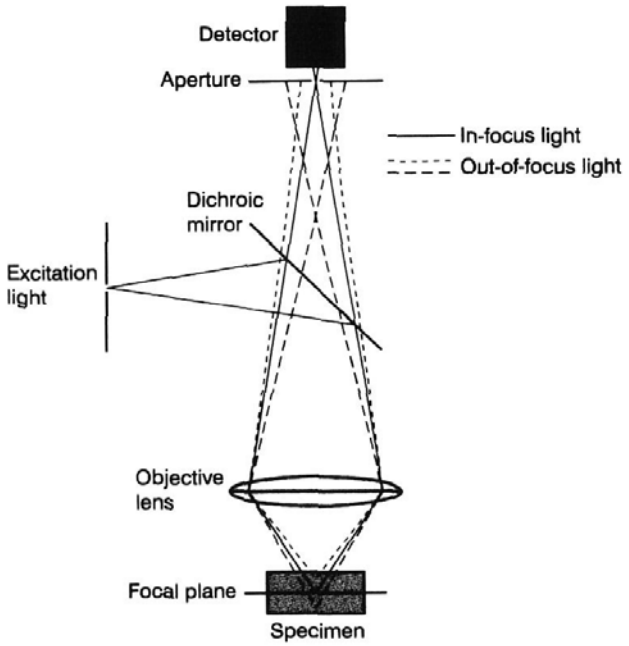


TEXT-FIGURE 1
Schematic illustration showing the basics of confocal laser scanning microscopy (after Wright *et al.* 1993). Excitation light, deflected to the objective lens by a dichroic mirror, is focused to a point on the plane of focus of the specimen. In-focus emissions (from the plane of focus - solid lines) retrace the incident light path and are directed by the objective lens through the aperture to the detector. Out-of-focus emissions (from above and below the plane of focus - dashed lines) do not follow the same path, so they are not focused through the aperture and are stopped from reaching the detector. The mirror is rapidly pivoted so that the point of light is scanned across the entire specimen.

ing from different viewpoints.

In the past CLSM has been utilised mainly by workers in the medical and biological sciences where it has proven an invaluable tool for studying both live and preserved specimens as it is a non-destructive technique (for examples see Matsumoto 1993). Recently, however, it has found favour in the Earth Sciences for studying such topics as fission tracks (eg. Petford and Miller 1993, 1995), fluid inclusions (eg. Petford and Miller 1993; Petford *et al.* 1994), chemical zonation in minerals (eg. Petford 1993) and microfractography of rocks (eg. Montoto *et al.* 1995). To the author's knowledge, the work presented herein is the first applying CLSM to the study of Radiolaria or any microfossils. For information on the history, technical aspects, types and applications of CLSM see Wilson (1990), Matsumoto (1993) and Lichtman (1994).

## APPLICATION OF CLSM TO RADIOLARIAN STUDIES

CLSM lends itself particularly well to the study of well preserved fossil Radiolaria. Previously, the only way to show internal structures of many Spumellaria clearly was with line drawings (eg. Haeckel 1887, pl. 41, figs. 2, 3, 6, 7; pl. 42, figs. 4-6, 9) - made with the aid of the conventional light microscope, and thus subject to the optical effects mentioned above which encourage artistic licence due to important details being obscured - or by physically sectioning the specimen (eg. Kozlova 1967), a destructive and time-consuming technique. Scanning electron microscopy (SEM) produces images with startling detail and clarity but one must find specimens that are broken in such a way as to enable the features required for study to be visible, or break them oneself, a very frustrating and time and labour-intensive exercise. SEM itself also requires much time-consuming preparation. CLSM enables clear views of diagnostic internal structures, shell cross-sections and surfaces unsurpassed by conventional light microscopy, it is non-destructive and requires no special sample preparation. To date the author has only trialed this technique on well-preserved Radiolaria of late Eocene to early Miocene age, so it is not known whether it can be effective with specimens of moderate to poor preservation. CLSM was found to work exceptionally well on lensoid and discoid Spumellaria. Although very few Nassellaria were investigated, preliminary results are encouraging in that area of study also.

Little sample preparation is necessary apart from the making of standard radiolarian strewn slides (eg. Moore 1973). The Radiolaria discussed below, and other well preserved specimens not documented here, fortuitously autofluoresced, ie. produced fluorescent emissions, under the laser without the need of stain to provide contrast for imaging or to make specimens visible (medical and biological specimens often need staining with a fluorescent dye or marker to enhance the visibility of areas of interest). Though the cause of fluorescence in the Radiolaria is not known it allowed the use of epifluorescence mode imaging using an excitation wavelength of 568nm with emissions of 590nm and greater collected for imaging. Reflectance mode imaging provided some surface information but was less successful for internal radiolarian imaging due to high internal reflection often obscuring areas of interest.

As images are stored on computer they can easily be manipulated. It is but a small task to adjust brightness, contrast or sharpness, for example, to enhance an image (see example 4, below). Stacks of optical sections, or *z* series, mentioned above, can be combined in the computer to render a three-dimensional image that can be tilted and rotated enabling viewing of the specimen from any angle. Stereo pairs can be generated in this way. Red/green stereo images can be produced from *z* series and viewed through special glasses to give a three-dimensional image which can be useful for showing the overall morphology of a specimen to an audience. This has been utilised herein, although the red/green images have been converted to greyscale. Information about the microscope objective used, the distance between optical sections, and other relevant data is saved along with the images, so measurements can be easily made in three dimensions on saved images. Plates are easy to construct from the saved images, thus bypassing time-consuming and messy photographic processes. If needed, images can be transferred to film or paper using conventional image transfer methods (eg. see Wright et al. 1993).

## EXAMPLES OF CLSM APPLIED TO RADIOLARIA

Eleven examples of CLSM applied to Radiolaria are given below, each comparing the information supplied via CLSM with that from transmitted light microscopy. Deficiencies in the CLSM technique are also noted. Plates illustrating CLSM images along with transmitted light photomicrographs (TLP) allow a visual comparison of the two techniques.

The CLSM images were taken at the Biomedical Imaging Unit, Department of Anatomy with Radiology, School of Medicine, University of Auckland with a Leica TCS 4D Confocal Laser Scanning Microscope utilising an Argon/Krypton mixed gas laser and using Leica's specialised software to run the system. Images were saved in TIFF format on a Silicon Graphics Iris Indigo XS24 computer, on which 3D renditions and other image analysis would normally be carried out, before being transferred to the Department of Geology where they were manipulated in Adobe Photoshop 3.0, saved as BMP images, imported into Corel DRAW! 4, resized, had scale bars etc. added, and were finally made into plates. Each image takes approximately 250Kb of disk space before any manipulation or enhancement. Transmitted light photomicrographs were taken in the Department of Geology with a Leitz Ortholux 2 Pol BK microscope and the resulting photographs scanned onto computer with a Microtek Scanmaker A3t scanner at 400dpi with the images then being treated as above. Plates were printed out on an Epson Stylus Pro XL printer.

**Example 1.** *Dictyocoryne truncatum* (Ehrenberg)
Plate 1, figures 1, 2

The TLP (pl.1, fig.1) shows only dark concentric rings in the central part of the specimen and it is virtually impossible to see if the arms are chambered or not. The CLSM image (pl. 1, fig. 2) clearly shows that there are three concentric shells in the central part, the outer two of which are divided. The arms are seen to be chambered only in their proximal parts, after which they become irregularly spongy.

**Example 2.** *Hymeniastrum* sp.
Plate 1, figures 3-5; plate 2, figures 9-16

As in Example 1, a comparison of the TLP (pl. 1, fig. 3) and the CLSM image (pl. 1, fig. 4, taken approx. 17µm below the surface) shows that the CLSM image provides much more information about the internal structure. Divisions within shells can be determined and the arms are seen to be chambered only in their proximal parts and spongy for most of their length. A combined *z* series of another specimen (pl. 1, fig. 5 - a black and white rendition of a red/green stereo image consisting of 8 op-

tical slices taken at 2.7μm intervals) shows that the innermost shell is spherical while the others are discoidal. The uncombined *z* series images are illustrated on plate 2, figures 9-16.

**Example 3.** *Rhopalastrum tritelum* O'Connor, in press A
Plate 1, figures 6, 7

In the original description of this species (O'Connor in press A) mention was made of the difficulty in making out the internal structure because of the dense patagium that is always present. The TLP (pl.1, fig.6) demonstrates this very well. The CLSM image (pl. 1, fig. 7, taken 28μm below the surface), however, shows three central chambers. It is also clear that the arms are of a more regular spongy structure than the patagium and that they are spongy all the way through. Note, however, that due to the very dense, spongy nature of the arms their distal parts are dark toward the centre. This may be due to the lack of excitation light penetrating to these areas (see conclusion). A similar phenomenon (although with conventional light) is seen in the TLP, but no detail at all can be discerned where it occurs.

**Example 4.** *Heliodiscus tunicatus* O'Connor, in press A
Plate 1, figures 8-10; plate 2, figures 23-37

The primary diagnostic feature of this species is the thin gown than envelopes the cortical shell (see O'Connor in press A). This feature is difficult to see in the TLP (pl. 1, fig. 8), appearing as a ragged edge to the cortical shell. The CLSM image (pl. 1, fig. 9; pl. 2, fig. 36, taken approx. 62μm below the surface) clearly shows the gown in cross-section as a thin band surrounding the cortical shell, and also shows spines connecting the two. In the TLP the medullary shells show as a dark patch in the centre of the specimen. The central part of the CLSM image has been enhanced (hence its speckled appearance) to show that there are two medullary shells. The enhancement was necessary because the information was extremely faint, probably due to the lack of excitation light penetrating the gown and thick-walled cortical shell (see conclusion). However, with the enhancement, the CLSM image provides important information on internal structure - much more than the TLP. The second CLSM image (pl. 1, fig. 10; pl. 2, fig. 30, taken approx. 38μm below the surface) shows the surface of the outer medullary shell and some of the spines that join it to the inside of the cortical shell. Although the centre of the image is faint (see above) some detail can still be made out and this information is unavailable under the transmitted light microscope. The full *z* series from which the above two CLSM examples are taken is also illustrated (pl. 2, figs. 23-37). It consists of 15 images taken at 4.8μm intervals starting at the surface. The two CLSM images discussed above are the 14th and 8th, respectively, in the *z* series.

**Example 5.** *Stylodictya validispina* Jörgensen
Plate 1, figures 11-13; plate 2, figures 17-22

The TLP (pl. 1, fig. 11) shows concentric rings and some radial spines but no real detail of internal structure. The combined *z* series (pl. 1, fig. 12 - a black and white rendition of a red/green stereo image, consisting of 6 optical slices taken at 2.4μm intervals starting just below the surface of the shell), however, gives a clear view of the internal structure, showing that each ring consists of many chambers, and while many spines radiate from the central undivided chamber to the margin, many also originate further out, subdividing distal but not proximal chambers, or proximal and distal chambers but not chambers between. The uncombined *z* series is also illustrated (pl. 2, figs. 17-22). Haeckel (1887, pl. 41, figs. 2, 3, 6, 7) illustrated the internal structure of several porodiscids but his drawings were done with the aid of conventional light microscopy and so may be considered open to artistic licence, ie. not true representations. Although not closely investigated, there seems to be no evidence of the girdle structures illustrated by Kozlova (1967, fig.1). The specimen appears to consist solely of concentric rings subdivided into chambers by radial spines and occasionally further divided by discontinuous spines. The second CLSM image (pl.1, fig.13, taken just below the surface) shows that the surface is composed of the external expressions of each ring, as described in Kozlova (1967, pg.1164).

**Example 6.** *Spongopyle osculosa* Dreyer.
Plate 1, figures 14-17; plate 2, figures 38-45

The TLP (pl.1, fig.14) only shows dark concentric rings and vague impressions of radial spines, while the CLSM image (pl.1, fig.15, taken approx. 43μm below the surface) clearly shows concentric shells and numerous radial spines extending from the central shell to the margin. A combined *z* series (pl.1, fig.16 - a black and white rendition of a red/green stereo image, consisting of 12 optical slices taken at 3.9μm intervals starting just below the surface of the shell) shows the central shell to be approximately spherical, while successive shells become progressively more flattened in the equatorial plane. Another CLSM image (pl.1, fig.17; pl.2, fig.38, taken approx. 12μm below the surface) shows the surface of one of the inner shells (centre) and cross-sections of the walls of some of the outer, enveloping shells, as well as many of the radial spines that join them. The uncombined *z* series is also illustrated (pl.2, figs.38-45 - the first CLSM image discussed above comes after the last illustrated image in the *z* series and the second one discussed is the first illustrated in the series).

**Example 7.** *Spongodiscus* ? sp.
Plate 1, figures 18-21

The TLP (pl. 1, fig. 18) of this species shows very little apart from vague concentric structure and what appear to be indistinct radial spines. The first CLSM image (pl. 1, fig. 19, taken approx. 28μm below the surface), however, shows a clear concentric structure of reasonably thick-walled shells, and that the radial spines of the TLP are really part of a regular spongy network, rather than discrete spines. The darkness of the centre of the CLSM image may be due to the lack of excitation light penetrating the many concentric shells (see conclusion), but it still gives more detail than the centre of the TLP, which only shows a vague, blurred area. A second CLSM image (pl.1, fig.21, taken 14μm below the surface) shows an inner shell at the centre and cross-sections of the walls of surrounding shells, information not available with a transmitted light microscope. A combined *z* series (pl.1, fig.20 - a black and white rendition of a red/green stereo image consisting of 10 optical slices taken at 2.8μm intervals) shows the regular, spongy structure of the species and its lensoid shape.

**Example 8.** *Spongotrochus antoniae* O'Connor, in press B.
Plate 1, figures 22-24

This species was originally described as having a bi-lobed central part with a peripheral disk consisting of a coarser spongy network (see O'Connor in press B). The first CLSM image (pl. 1, fig. 22) shows this clearly. In the second CLSM image (pl. 1, fig. 24) there appears to be a globular, thickened central mass not visible in the TLP (pl. 1, fig. 23). This additional information may exclude *S. antoniae* from *Spongotrochus*, as the generic

definition was applied in the sense of Petrushevskaya (1974, p.574) to forms with a central thickened mass, the central part of which is not globular.

**Example 9.** *Lithelius* ? sp.
plate 2, figures 1, 2

This is one case where the TLP (pl .2, fig. 1) provides information not seen in the CLSM image (pl. 2, fig. 2, taken approx. 14μm below the surface). The TLP image shows concentric shells from the centre to the periphery. The central part of the CLSM image is dark, possibly because of the lack of excitation light penetrating the many concentric shells (see conclusion). However, the CLSM image clearly shows that each concentric shell is divided by spines radiating from the centre to the periphery, a feature only vaguely visible in the TLP.

**Example 10.** *Stylatractus* ? sp.
Plate 2, figures 3-6

In the TLP (pl. 2, fig. 3) three concentric shells can be vaguely distinguished but little other information is visible. The first CLSM image (pl. 2, fig. 4, taken approx. 53μm below the surface) clearly shows three concentric shells, along with some of the radial spines that join them, and the pyriform shape of the inner medullary shell is clear. Note, also, zoning in the polar spine that may represent growth phases of the spine. The second CLSM image (pl. 2, fig. 5, taken approx. 13μm below the surface) shows the surface of the outer medullary shell (centre) and some of the radial spines joining it to the inside of the cortical shell. The third CLSM image (pl. 2, fig. 6, taken approx. 31μm below the surface) shows the surface of the inner medullary shell along with a few of the radial spines joining it to the inside of the outer medullary shell and many of the radial spines joining the outer medullary shell to the inside of the cortical shell. Note, again, zoning of the polar spine. The lack of detail of the inner medullary shell may be due to the low level of excitation light penetrating the first two shells (see conclusion), but there is still enough information to make this a useful view. TLPs show none of this detail.

**Example 11.** *Siphocampe grantmackiei* O'Connor, in press B.
Plate 2, figures 7, 8

This is the only Nassellaria investigated herein but these preliminary results show that there is potential for this method in nassellarian studies. Little internal detail can be seen in the TLP (pl. 2, fig. 7, taken through the sagittal plane). The CLSM image (pl. 2, fig. 8, taken through the sagittal plane), however, shows the presence of a group of long axial spines, only vaguely visible on the TLP. Other internal skeletal structures clearly visible on the CLSM image include **D**, **A**, **M**, **V** and **Vs** (terminology after O'Connor in press A). Although some of these structures can be discerned under the transmitted light microscope they are generally very vague and nowhere near as clear as with CLSM.

## PLATES

The specimens illustrated in the following plates came from two samples - an Early Oligocene sample from Matakohe Quarry, Northland, New Zealand (New Zealand Fossil Record Number Q08/f555 - see O'Connor 1993, 1994, in press A) and an Early Miocene sample from Te Kopua Point, Kaipara Harbour, Northland, New Zealand (New Zealand Fossil Record Number Q08/f569 - see O'Connor in press A, B). The **Rnnn** number associated with each specimen refers to its place in the University of Auckland Department of Geology Catalogue of Type and Figured Specimens. All samples and specimens are lodged with the Department of Geology, University of Auckland. For more information on figures see associated examples in the text.

### PLATE 1

Figures 2, 4, 5, 7, 9, 10, 12, 13, 15-17, 19-22 and 24 are confocal laser scanning microscope images;
Figs.1, 3, 6, 8, 11, 14, 18 and 23 are transmitted light photomicrographs.
Specimens in figs.1-5 and 11-24 are Early Miocene in age from Te Kopua Point (sample Q08/f569);
specimens in figs.6-10 are Early Oligocene in age from Matakohe Quarry (sample Q08/f555). All scale bars are 50μm.

1,2 *Dictyocoryne truncatum* (Ehrenberg). 1, R355; 2, R356.

3-5 *Hymeniastrum* sp. 3-4, R357; 5, R358, combined *z* series.

6,7 *Rhopalastrum tritelum* O'Connor. 6, R140; 7, R359, arrows indicate the three concentric shells.

8-10 *Heliodiscus tunicatus* O'Connor. 8, R130; 9-10, R360; 9, upward directed arrow indicates gown, downward directed arrow indicates outer medullary shell, horizontal arrow indicates inner medullary shell.

11-13 *Stylodictya validispina* Jörgensen. 11, R361; 12-13, R362; 12, combined *z* series.

14-17 *Spongopyle osculosa* Dreyer. 14, R363; 15-17, R364; 16, combined *z* series.

18-21 *Spongodiscus* ? sp. 18-21, R365; 20, combined *z* series.

22-24 *Spongotrochus antoniae* O'Connor. 22, R366; 23, R245; 24, R367.

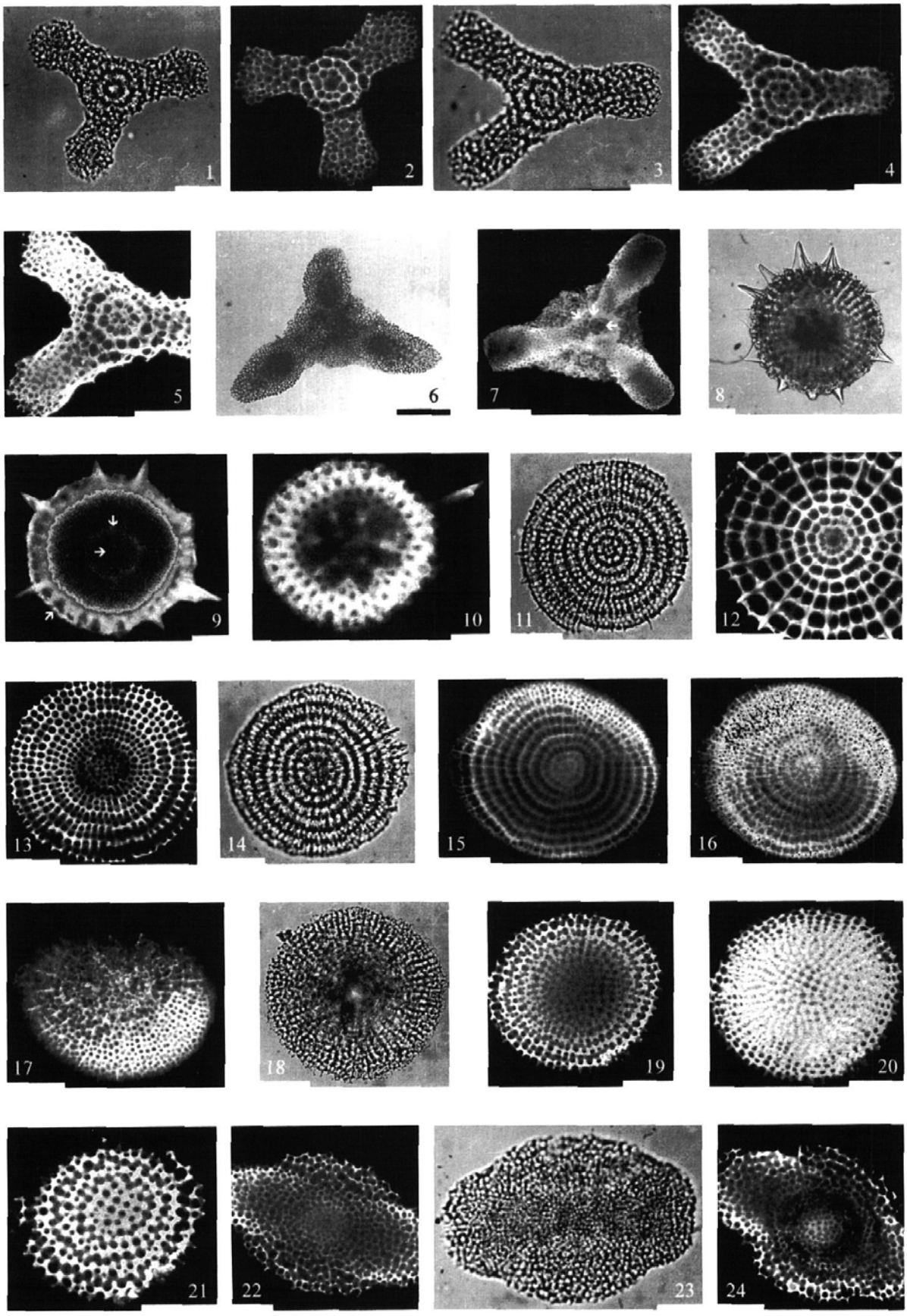
1
2
3
4
5
6
7
8
9
10
11
12
13
14
15
16
17
18
19
20
21
22
23
24

## CONCLUSION

Although CLSM is an extremely useful technique, and one which should become an integral part of radiolarian studies in the future, its use in this field is still in the fledgling stages. For example it is still to be determined whether only well preserved specimens autofluoresce and if so can moderately or poorly preserved specimens still be imaged to any extent. It must also be remembered that for all its usefulness CLSM is still a technique that utilises light and so is subject to a few of the problems plaguing conventional light microscopy. This is evident in some specimens with many concentric shells, and in some thick-shelled or densely spongy specimens, where the internal structures are very dim or cannot be seen at all. The lack of internal information may be due to light reflection at the specimen surface and within the specimen, and also light absorption by the overlying shells. This reflection and absorption means that little light reaches the central parts of these specimens so detectable emissions are very low or non-existent. Problems with refraction and spherical aberration may also be encountered (see Majlof and Forsgren 1993). The fact that CLSM is not available to all radiolarists could restrict its usage somewhat.

These inadequacies, however, are vastly outweighed by the amount of information available through CLSM and it cannot be ignored as an important additional source of information for radiolarian studies. The use of CLSM in conjunction with standard transmitted light microscopy (still the main means of radiolarian illustration and identification, due mainly to its availability) and SEM (unsurpassed in producing high quality, detailed surface images at all magnifications) can only enhance the degree of information available on many radiolarian taxa, enabling clarification of often confusing and incomplete radiolarian taxonomy.

## ACKNOWLEDGMENTS

Many thanks are due to Dr Colin Green of the Anatomy Department, School of Medicine, University of Auckland, without whose expert help this work would not have been possible. His many hours of help and enduring patience over minor requests and constant rescheduling of CLSM time are greatly appreciated. Thanks also to John Nowak for safely transferring the image files from the Biomedical Imaging Unit's computer system to that in the Geology Department and for allotting me vast amounts of disk space for storing and manipulating the images.

Thank you to Associate-Professor Kerry Rogers of the Geology Department who first introduced me to CLSM and continued to encourage me to make use of it, and to Associate-Professor Jack Grant-Mackie for his encouragement and proof reading of the various drafts of the manuscript. This study was made possible, in part, with the aid of a University of Auckland Doctoral Scholarship and the McKee Trust Postgraduate Scholarship.

## REFERENCES

HAECKEL, E., 1887. Report on the Radiolaria collected by *H.M.S. Challenger* during the years 1873-76. Report on the scientific results of the voyage of the *H.M.S. Challenger*, Zoology 18. Two parts, clxxxviii + 1803pp., 140 pls., 1 map.

KOZLOVA, G.E., 1967. Tipy stroeniya radiolarii iz sem. Porodiscidae (Types of skeletal structure in the family Porodiscidae). Zool. Zhurn. t. 46, vyp. 8:1163-1172

LICHTMAN, J.W., 1994. Confocal Microscopy. Scientific American, August 1994:30-35.

MAJLOF, L and FORSGREN, P., 1993. Confocal microscopy: important considerations for accurate imaging. In: Matsumoto, B. (ed). Cell Biological Applications of Confocal Microscopy. Methods in Cell Biology, Volume 38. Academic Press, San Diego. pp79-95.

MATSUMOTO, B. (ed), 1993. Cell biological applications of confocal microscopy. Methods in Cell Biology, Volume 38. Academic Press, San Diego. 380pp.

MONTOTO, M., MARTÍNEZ-NISTAL, A., RODRÍGUEZ-REY, A., FERNÁNDEZ-MERAYO, N. and SORIANO, P., 1995. Microfractography of granitic rocks under confocal scanning laser microscopy. Journal of Microscopy, 177:138-149.

MOORE, T.C.jr., 1973. Method of randomly distributing grains for microscopic examination. Journal of Sedimentary Petrology, 43:904-906.

O'CONNOR, B.M., 1993. Radiolaria from the Mahurangi Limestone, Northland, New Zealand. Unpublished M.Sc. thesis, Department of Geology, University of Auckland. 135pp.

————, 1994. Seven new radiolarian species from the Oligocene of New Zealand. Micropaleontology, 40:337-350.

————, in press A. New Radiolaria from the Oligocene and Early Miocene of New Zealand. Micropaleontology.

---

## PLATE 2

Figures 2, 4-6 and 8-45 are confocal laser scanning microscope images; figs. 1, 3 and 7 are transmitted light photomicrographs. Specimens in Figs.1-22 and 38-45 are Early Miocene in age from Te Kopua Point (sample Q08/f569); specimen in figs.23-37 is Early Oligocene in age from Matakohe Quarry (sample Q08/f555). All scale bars are 50µm.

1,2 *Lithelius* ? sp. 1, R368; 2, R369.

3-6 *Stylatractus* ? sp. 3-6, R370; 4, 6, arrows indicate zoning within polar spines.

7,8 *Siphocampe grantmackiei* O'Connor. 7, R371; 8, R372; 7, 8, arrows indicate axial spines.

9-16 *Hymeniastrum* sp. 9-16, R357, *z* series from just below surface downward.

17-22 *Stylodictya validispina* Jörgensen. 17-22, R362, *z* series from just below surface downward.

23-37 *Heliodiscus tunicatus* O'Connor. 23-37) R360, *z* series from surface downward.

38-45 *Spongopyle osculosa* Dreyer. 38-45, R364, *z* series from just below surface downward.

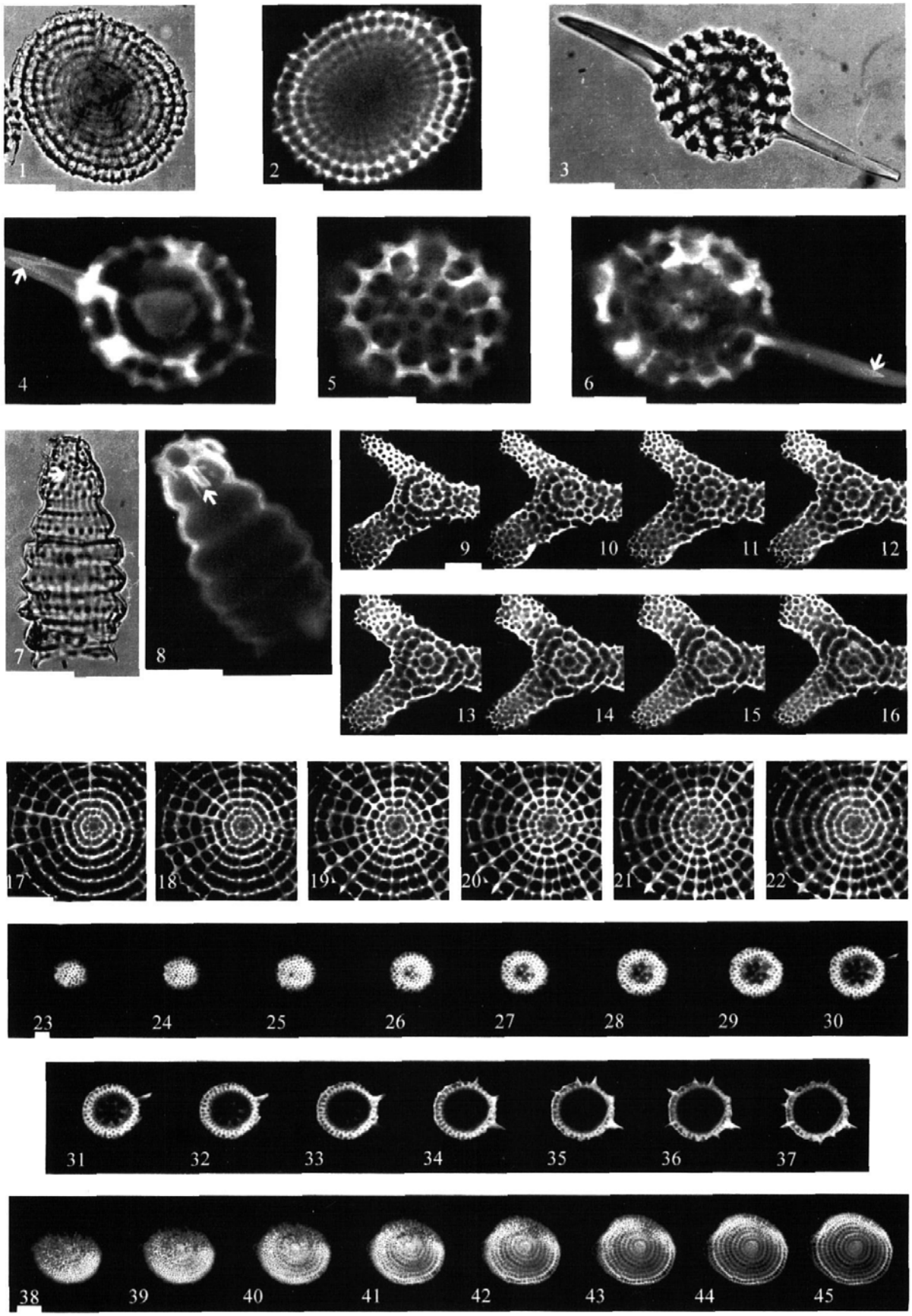
1
2
3
4
5
6
7
8
9
10
11
12
13
14
15
16
17
18
19
20
21
22
23
24
25
26
27
28
29
30
31
32
33
34
35
36
37
38
39
40
41
42
43
44
45

————, in press B. Lower Miocene Radiolaria from Te Kopua Point, Kaipara Harbour, New Zealand. Micropaleontology.

PETFORD, N., 1993. Mineral studies using confocal scanning laser microscopy. Microscopy and Analysis, September 1993:19-21.

PETFORD, N. and MILLER, J.A., 1993. The study of fission track and other crystalline defects using confocal scanning laser microscopy. Journal of Microcopy, 170:201-212.

————, 1995. Some aspects of the application of image analysis to the study of fission tracks. Mineralogical Magazine, 59:197-201.

PETFORD, N., MILLER, J.A. and RANKIN, A.H., 1995. Preliminary confocal scanning laser microscopy study of fluid inclusions in quartz. Journal of Microscopy, 178:37-41.

PETRUSHEVSKAYA, M.G., 1974. Cenozoic radiolarians of the Antarctic. In: Kennett, J.P. *et al.* Initial Reports of the Deep Sea Drilling Project, Volume 29:541-675. US Government Printing Office, Washington.

WILSON, T., (Ed), 1990. Confocal Microscopy. Academic Press, London. 426pp.

WRIGHT, S.J., CENTONZE, V.E., STRICKER, S.A., DE VRIES, P.J., PADDOCK, S.W. and SCHATTEN, G., 1993. Introduction to confocal microscopy and three-dimensional reconstruction. *In:* Matsumoto, B. (ed). Cell Biological Applications of Confocal Microscopy. Methods in Cell Biology, Volume 38. Academic Press, San Diego. pp1-45.

Manuscript received January 25, 1996
Manuscript accepted February 9, 1996